Bulletin of Electrochemistry 19 (7) July 2003, pp 319-334

0256-1654/2003/$ 3-50
© 2003 CECRI

COMBUSTION SYNTHESIS OF ABO_3 AND AB_2O_4 COMPOUNDS - AN OVERVIEW

C O AUGUSTIN* AND R KALAI SELVAN

* *Central Electrochemical Research Institute, Karaikudi 630 006. INDIA*
Department of Materials Science, Madurai Kamaraj University, Madurai 625 021. INDIA.

[Received: 31 January 2003 Accepted: 20 February 2003]

Combustion synthesis has been accepted as a versatile method to synthesize new materials due to its simplicity. The method has been used to prepare numerous materials among which perovskites (ABO_3) and spinels (AB_2O_4) occupy a prominent place. An attempt has been made in this overview to consolidate the recent works on combustion synthesis of these new materials. Various experimental conditions to synthesize the required products and different characterization tools used for unraveling the structural features are highlighted. Further the novelty and mathematical basis of preparative conditions for the synthesis employed by different researchers are also enumerated. This covers the salient features of synthesis, property evaluation and applications of simple as well as substituted perovskite and spinel compounds carried out recently. This will be useful to any researcher entering into this field of new materials world.

Keywords: Combustion synthesis, perovskites, spinels.

INTRODUCTION

Combustion by definition is consumption by fire, development of heat or light from chemical combination of substances with oxygen. Synthesis means artificial production of new compounds from their constituents. Broadly, combustion synthesis may be considered as a preparation process to produce homogeneous, very fine, crystalline, unagglomerated multi component oxide ceramic powders without the intermediate decomposition and/or calcining steps. This is a non-conventional method for materials synthesis, which makes use of an exothermic chemical reaction. These processes rely on a balance between the heat generated and dissipated in chemical reactions. It involves mixing of different reactant powders, such as metals, metal oxides, and nonmetals, which on initiation produce exothermic chemical reaction that is self-sustaining due to a positive energy balance. The reactants produce rapid heating and cooling which aids propagation by a combustion wave that moves out from the source of initiation. Two relatively new synthetic variants have been developed which negate the need for external heating. These are based on self- propagating reactions, which provide the energy to overcome the solid-state diffusion barrier internally, within the starting materials by promoting exothermic chemical reactions. These processes are termed as self-propagating high temperature synthesis (SHS) or solid-state metathesis (SSM).

Alexander G Merzhanov, I P Borovinskaya and V M Shkiro have first discovered the novel method of synthesis at the research center of USSR, Academy of sciences in Russia in the year of 1967. At that time the process was named as "The phenomenon of the wave localization of solid-state auto retarding reactions". Later during 1980s the full potential of the combustion synthesis has been developed by American scientists, subsequently various teams around the world in France, China, Italy, India, Poland, Korea, Spain, Japan and Israel have adopted this unique process for the synthesis of many new materials totaling around

* Author for correspondence
e-mail - caugustin@rediffmail.com , Fax: 04565-227779, 227713

1000, covering mixed oxides, carbides, nitrides, silicides, borides, intermetallics etc. with the aim of end applications in sensitive and specific areas such as nuclear, magnetic, space, metallurgy, semiconductors, insulators, sensors, catalysts, phosphors, and superconductors. The combustion method is a continuous process for the production of advanced materials making use of the heat energy generated by the exothermic reaction activated within the reactants and simultaneous propagation of a combustion wave along the whole materials. Large quantities of high pure materials can easily be synthesized cost effectively without high temperature and complex processing equipments within short time. A number of synthetic routes have been adopted for the preparation of new materials like conventional ceramic method, sol-gel method, co- precipitation process, hydrothermal synthesis and electrochemical method. Salient features of the above processes are summarized below.

Sol-gel method

Sol-gel method is coming under the category of wet chemical process. Sol-gel resources the solutions i.e. the starting precursors like metal alkoxides, metal oxalates etc have been converted into gel form using some gelating agents like 2-ethyl- 1hexanol due to the increase in viscosity. The following important steps are included in the synthetic process such as hydrolysis, polymerization, gelation, drying, dehydration and densification. Using this process, large number of new materials $SrAl_2O_4$ [1], $SrZrO_3$ [2-3], Ca doped $LaMnO_3$ [4] have been prepared. Citric acid [5] and Poly Acrylic acid [6] are also used as the gelating agents.

Co-precipitation method

In this method the metal nitrate salts are preferred as starting precursors due to their solubility in water and the nitrate salts are co-precipitated in a common medium usually as hydroxides. It is important that the solid precipitating out is really insoluble in the mother liquor. The precipitate after drying is heated to the required temperature in a desired atmosphere to get the final product. The spinel, $NiFe_2O_4$ [7-8] has been prepared by this method.

Hydrothermal process

In this process the reactants taken in the form of metal nitrates/acetates or hydroxides salts are mixed to form a hydrous gel which is then converted into a precipitate under pressure using autoclave for several hours. Then the precipitate was filtered and washed with distilled water and ethanol to remove the byproduct and the impurities. The $ZnAl_2O_4$ spinel [9] and $LiNbO_3$ perovskite [10] have been prepared using this method.

Electrochemical method

In this method different types of materials such as metals, ceramics, semiconductors, conducting polymers etc have been prepared. It is a single step method. In this method product species is present in the electrolyte which undergoes reduction. The following ferrite materials $CuFe_2O_4$ [11], $NiFe_2O_4$ [12] and $CoFe_2O_4$ [13] have been prepared.

Characteristics of combustion synthesis

Combustion synthesis (CS) is a very fast solid flame combustion method with release of gases to give high pure solid product. This process consists of initiation, propagation and termination.

Initiation is low calorie reaction taking place at the surface of the reactants with introduction of heat flux either by a hot wire, electric spark or laser beam. The reaction may also be initiated by bulk heating in a furnace, hot plate or in an open flame, which is carried out in the mode of thermal explosion. An auto wave process and induction process are the two methods generally adopted for initiating combustion synthesis. The essential difference between the two is that in the former, a momentary local heating takes place by combustion wave starting chemical reactions leading to the product formation. Whereas, in the

latter a continuous heating through entire material takes place via a warming up by thermal explosion aiding the stipulated chemical reactions and product formation. Propagation is the second stage in combustion synthesis in which all the wave points initiated move at a constant speed to the thermal release zone to transform the reacting materials in to the final products after structuralization and termination of the synthesis reaction. The optimum conditions required for the combustion synthesis are listed in Table I.

Combustion synthesis involves calculations based on many mathematical equations for finding out energy balances, reaction rate, propagation velocity, combustion temperature, time etc of which some are given below [14].

The energy equation for transient heat conduction, including the source term, containing heat release due to the exothermic combustion reaction is given as

$$\rho C_p \frac{\partial T}{\partial t} = K \frac{\partial T^2}{\partial t^2} - \frac{4h(T - T_0)}{d} + \rho Q (1 - M_{FC}) \Phi(T,\eta) \quad (1)$$

The reaction rate

$$\Phi(T,\eta) = \frac{\partial \eta}{\partial t} = K_0 (1 - \eta) \exp\left(\frac{E}{RT}\right) \quad (2)$$

TABLE I: Optimum conditions of combustion synthesis

Properties	Unit	Values
Combustion temperature	K	1773-4273
Wave propagation rate	cmS^{-1}	0.1-20
Rate of heating	$^0C/S$	10^3-10^6
Initiation time	Sec	0.1-4
Initiation intensity	$Cal.cm^{-2}.sec^{-1}$	10-200
Initiation temperature	K	573-973
thickness of reaction zone	mm	0.1-5

The propagation velocity has been reported to be a function of the combustion temperature

$$p^2 = \frac{1}{f(\rho Q / K)} \times \frac{K_0 R T_c^2}{2E} \exp\left(\frac{-E}{R t_C}\right) \quad (3)$$

The length of reaction zone (l_r) and pre heat zone (l_p) related to the activation energy (E) and combustion temperature (T_c) can be expressed as

$$\frac{l_r}{l_p} \alpha RT_c / E \quad (4)$$

where C_P is heat capacity ($J\,Kg^{-1}\,K^{-1}$); E is activation energy ($J\,mol^{-1}$); K is thermal conductivity ($J\,m^{-1}\,S^{-1}\,K^{-1}$); K_0 is pre-exponential factor (S^{-1}); MFC is Molar fraction of diluents present at any η; P is Porosity (%); Q is Exothermic heat of reaction ($J\,mol^{-1}$); T is Temperature (K); T_C is Combustion temperature (K); T_0 is Initial temp. of unreacted compacts (K); T_η is boundary temperature (K); Z is dimensional co-ordinate (m); d is diameter of the specimen; h is surface heat transfer co-efficient ($J\,m^{-2}\,K^{-1}\,S^{-1}$); t is time(s); ρ is density (Kgm^{-3}); η is fraction reacted; $\varphi(T, \eta)$ is reaction rate (S^{-1}).

Novelty

- This is a non-conventional method for material synthesis, which makes use of exothermic chemical reactions.
- More economical in terms of energy expenditure compared to the conventional ceramic method.
- It is very fast and simple due to the absence of any intermediate steps.
- Large quantities of high purity new materials can be prepared rapidly and at reduced cost.
- The need for high temperature furnaces and complex processing equipment is eliminated.
- Very low processing temperature.
- It gives a homogenous product with high surface area, well- defined chemical compositions and homogeneous distribution of elements.

¤ Energy consumption is greatly reduced.

Areas of application

Combustion-synthesized products have been used as abrasives, high temperature heating elements, electrodes, solid lubricants, semiconductor materials and polishing pastes. This technology has been used to apply various protective coatings to metal substrates in diverse applications such as the production of N & P fertilizers. Other potential applications are the production of non ferrous metal powders, the direct reduction of ferrous ores to Fe and the smelting of high alloy, high temperature metals. High thermo mechanical properties of the powder materials produced by the process have great strength, thermo-wear resistance and good corrosion stability. In turn have broad range of applications in metal cutting tools, alloying additives in metallurgy, parts of nozzles, turbines in air craft, coating of turbine

Table II: Applications of some ABO_3 and AB_2O_4 compounds

Sl No	Materials	Specific properties	Applications
1.	$LaNiO_{3-\delta}$	High metallic conductivity, Pauli-paramagnetism and very high electrocatalytic activity particularly in oxygen reduction processes.	*Electrodes in electrochemical devices such as SOFC, and MCFCs*
2	$CaTiO_3$	Porous and high nuclear cross section	*Nuclear waste immobilization*
3	$RFeO_3$, $RCrO_3$ (R-Rare earth elements)	An unusual variety of magnetic properties and structural changes	*Resonance based devices such as logic and memory element, lasers and light modulators in optical applications. Catalytically active for the complex oxidation of hydrocarbons, combustion catalysts as well as sensors and solid electrolytes*
4	$LaMnO_3$ and $LaCoO_3$	Intrinsic p-type conductivity and shows large oxygen deficiency at higher temperatures	*SOFC cathode materials*
5	$LaAlO_3$	Dielectric properties	*Buffer layer in super conductor applications*
6	$BaTiO_3$	Dielectric properties	*Piezo electric ceramic material*
7	$LaMn_{1-x}Co_xO_3$	Linear thermal expansion and conductivity	*SOFC cathdoe material*
8	$Ln_{1-x}MnO_3$ (Ln = Pr, Nd & Sm)	High surface area of 13-40 m^2/ g. The thermal expansion coefficients of substituted compounds are very close to that of the electrolyte (YSZ) used in SOFC	*SOFC cathode material*

Table II contd

Table II: Contd

Sl No	Materials	Specific properties	Applications
9	$Sr(Fe_{0.5}Ti_{0.5})O_3$	Structural and electrical properties	*Electrochemical applications such as semipermeable membranes, electrodes, interconnector materials in SOFCs and resistive gas sensors*
10	$MgAl_2O_4$	It melts congruently at 2408 K, shows high resistance to attack by most of the acids and alkalis and has low electrical losses	*Refractory in lining of steel-making furnaces, transition and burning zones of cement rotary kilns, checker work of the glass furnace regenerators, sidewalls and bottom of the steel ladles, glass furnaces and melting tanks*
11	$MgIn_2O_4$	The optical transmittance is much higher than that of ITO in the blue region (400-500 nm)	*LCDs and photo electronic devices*
12	$LiMn_2O_4$	The charge discharge curves showed two plateaux with the charge density of 107 $mAhg^{-1}$	*Cathode material in lithium batteries*
13	MFe_2O_4, (Cu, Ni, Zn & Co)	Microwave absorption	*Sensor elements*
14	$BaFe_{12}O_9$	It is a hard magnetic material with a maximum coercivity of 4800 Oe, high recording density and low manufacturing costs	*Advanced magnetic recording applications such as high definition video and flexible discs*
15	$SrFe_{12}O_{19}$ and $PbFe_{12}O_{19}$	Magnetic properties	*Permanent magnets and as the magnetic strips on credit/ debit cards*
16	$Li_{0.5}Fe_{2.5}O_4$	It is soft ferrite with a very high Curie temperature of 911 K	*Microwave and Memory core devices*
17	$Mg_{0.5}Zn_{0.5}Fe_2O_4$	High saturation magnetization of 59.3 emu g^{-1} and low coercivity	*Television sets, focusing systems and high frequency cellular telephones*

blades, automobile construction and piezo-electrics in electronic fields. Table II explains the specific properties and applications of the some of the spinel and perovskite compounds.

Combustion synthesis has been in the limelight for over three decades and many have reviewed the status of the process from time to time. A G Merzanov [15], one of the pioneers of combustion

synthesis has analyzed various developments and applications. And modelling has been made by Bowen [16-17] and Yi *et al.* [18]. Moore and Feng [19] had explained the historical developments and the parameters that control the synthesis method and their applications. The advanced materials prepared by combustion synthesis have been overviewed by many authors [20- 25].

Mixed oxide materials with spinel and perovskite structures possessing high electrical conductivity, electrocatalytic activity, thermal and mechanical stability have been identified as oxygen evolving green electrode for metallurgical operations. Hence, the rejuvenated interest in these materials, which prompted this attempt. In this overview, an outline, novelty, mathematical background and applications are presented. Further the versatility of this unique process in the synthesis of two important classes of compounds namely; perovskites (ABO_3) and spinel (AB_2O_4) are highlighted. This gives an insight into various synthetic conditions for the preparation of different materials, with various structures and characteristics.

Perovskite Structure (ABO_3)

The ideal perovskite structure, ABO_3 , is of cubic ($Pm\bar{3}m$) symmetry and can be described as a three dimensional network of corner sharing BO_3 octahedra. The 'A' cation is in the center of a cube defined by eight of these octohedra. Comparatively few perovskites have the ideal cubic structure with B-O-B angles of 180^0; most bear some extent of distortion. The symmetry of perovskite depends upon the relative size and electronic configuration of cations occupying A or B sites. The stability of these structures could be predicted as a function of ionic sizes and the tolerance factor. The tolerance factor, $t = (r_A + r_0)/ \sqrt{A_2 (R_B + r_0)}$ where r_A, r_B and r_0 are ionic radii of the 'A' & 'B' cations and the 'O' anions respectively. The detailed features of the perovskite ($CaTiO_3$) structure are exhibited in Fig. 1. Each titanium atom is octahedrally coordinated with six oxygen atoms and a calcium atom in the center.

Simple perovskites

Metallic chromites, ferrates, manganates and cuprates are some of the class of materials prepared by combustion synthesis. Morelli *et al.* [26] had synthesized $LaCrO_3$ powders, and compared the properties with that from alternative chemical route and solid-state method. The structural and morphological characteristics were studied by XRD, SEM and TEM. They have reported that the prepared fine powders were uniform in particle size, which increased with sintering. Jung *et al.* [27] had reported that the *p*H of solution did not influence the morphological features but affected the combustion product. It has been reported that when the *p*H of solution was in the range 0.7 to 4, the yield of the product was more than 90%. Zupan *et al.* [28] have reported that the specific surface area of the combustion product of $LaCrO_3$ using microwave induced heating method was larger (25-32 m^2/ g) than that of hot plate heating method (10-14 m^2/ g). The physical and chemical properties were evaluated and the maximum theoretical density has been obtained at 1573 K. Nanocrystalline $LaFeO_3$ had been prepared from nitrate salts and citric acid as precursors [29]. It has been reported that citric acid plays two important functions, one is as chelating agent and the other is to provide the fuel for auto ignition temperature. The synthesized materials have the particle size of 30 nm. The magnetic studies were

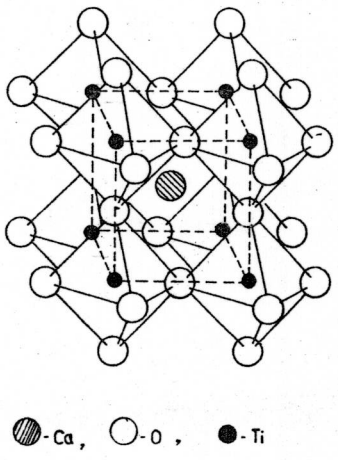

Fig. 1: Perovskite Structure ($CaTiO_3$)

also carried out; the coercivity of the nanocrystalline $LaFeO_3$ was 98.82G and the value of saturation magnetization was 2.75 $emu.g^{-1}$, which was lower in comparison with other nanocrystalline MnCuZn ferrites (48.813 $emu.g^{-1}$).

Stevenson *et al.* [30] had reported that the electrical conductivity and thermal expansion of the materials (La, Sr) (Ga, Mg, Cu, Co, Fe) $O_3-\delta$ increased substantially with increasing cobalt content and the thermal expansion of the iron doped compounds increased slightly with increasing iron content except for the composition with the highest amount of iron. Aguas *et al.* [31] had synthesized lithium and sodium niobates and tantalates ($LiNbO_3$, $LiTaO_3$, $NaNbO_3$ and $NaTaO_3$) by combustion and sol-gel methods using metal oxide precursors by the addition of methanol.

The piezo electric ceramic material $BaTiO_3$ had been prepared and characterized using various methods by Zhu *et al.* [32]. Lanthanides such as La, Gd and Ce have been recognized as elements present in the radioactive waste which were immobilized by forming solid solutions with $CaTiO_3$. The combustion synthesized powders have a good sinterability with the linear shrinkage of > 25% up to 1773 K, while that prepared by solid state method have < 10% under the same conditions. Nanosized powder of $SrTiO_3$ have been prepared using metal nitrates and differing the amounts of EDTE as reducing and NH_4NO_3 as oxidizing reactants by Poth *et al.* [33]. Nanocrystalline $SrTiO_3$ powders were characterized using XRD and FTIR spectra at various sintering temperatures 1073 to 1273 K. These spectra showed the grain growth velocity and the existence of different $SrCO_3$ species [34].

Mao *et al.* [35] had prepared the $LaAlO_3$ powder using metal nitrates and oxalildihydrazide. The combustion product at 623 K was amorphous whereas a single phase perovskite was obtained at 773 K. DSC analysis on the mixture showed that the combustion started at 613 K. X-ray diffraction data showed that the product had crystallite size up to 42 nm. Crystallites size distribution was confirmed by TEM images. A thorough study of $MSnO_3$ (M = Ca, Sr and Ba) compounds with respect to their synthesis, processing and microstructural characterization has been made in a recent work [36-37]. A well-defined microstructure with small grain size (~1(m) and near zero porosity could be obtained by select sintering schedule of 1623 K/t h (48 h < t ≤ 60h) for $CeSnO_3$ sample.

Mixed perovskites

Mixed perovskites are obtained from simple ones by substitution of one or more of metallic elements in the A or B sites. Strontium doped $LaCrO_3$ samples have been synthesized using metal oxides and sodium perchlorate acting as fuel. The reaction conditions and the microstructure formation have been studied and reported [38-39]. These compounds are used as inter connectors in solid oxide fuel cells due to their thermodynamic feasibility. The oxidation of Cr is the main source of heat generation for maintaining a stable reaction front. Replacing part of the metallic chromium in the reaction mixture by its oxide may modify the combustion temperature, propagating velocity and product particle size. The predicted and observed combustion temperatures were in reasonable agreement. Zupan *et al.* [40] have proposed that one of the most important components for the Solid Oxide Fuel Cells (SOFC) is the separator material, which is doped with alkaline earth cations (Mg, Ca, Sr or Ba) are substituted for a fraction of A or B lattice sites in $LaCrO_3$ perovskite. He reported that the sinterability in air is improved by the substitution of calcium (LCC) or strontium (LSC) in $LaCrO_3$. This is carried out by the gel combustion synthesis rather than other synthetic methods. LCC powders could be densified to high relative density 98% after sintering at 13273 K, while for the densification of LSC much higher temperature was required (16273 K). The economic production of $La_{1-x}Sr_xCrO_3$ and $La_{1-x}Sr_xMnO_3$ from the oxide powders of the corresponding metals and metal oxides of Cr & Mn was made by Ming *et al.* [41]. The predicted and observed combustion

temperatures were in reasonable agreement. The strontium substituted $LaCrO_3$ has been prepared by Kuznetsov *et al.* [42]. The parameters of the process in chemical reaction, intermediate phases as well as structures and properties of the synthesized product were also investigated. Lanthanide ortho chromites of general formula $LnCrO_3$ (Ln = La, Ca, Pr, Nd, Sm, Eu, Tb, Dy, Ho, Er, Tm, Tb, Lu) have been prepared with the maximum reaction temperature (Tc) and the propagation velocity values were measured for all samples. Systematic changes in the lattice parameters, cell volume and pycnometric densities were correlated with the atomic number of the lanthanide. SHS prepared $LnCrO_3$ samples were shown to be weak antiferromagnets. IR refection spectra for $LnCrO_3$ materials gave 4 broad absorption bands in the region of 800-200 cm^{-1} [43]. Pure and Cr substituted lanthanum orthoferrites $LaFe_{1-x}Cr_xO_3$ (x = 0, 0.1, 0.25, 0.4, 0.55, 0.7, 0.85, 1) have been synthesized and SEM, EDAX and XRD, IR, UV/Visible spectroscopic experiments were carried out by Maxim *et al.* [44]. These results indicated that the SHS route was a potentially useful means of synthesizing orthoferrities with desirable properties.

Effect of sintering on the electrical conductivity and thermal expansion behavior of combustion synthesized strontium substituted rare earth manganites with the general formula $Ln_{1-x}Sr_xMnO_3$ (Ln = Pr, Nd and Sm; X = 0, 0.16 and 0.25) have been investigated by Aruna *et al.* [45]. The surface area of the rare earth manganites was 13-40 m^2/ gm. The electrical conductivity values increased with increase in the substitution of strontium. With the decreasing ionic radii of rare earth ions, the conductivity value decreased. Among the rare earth manganites studied (Pr/Nd) 0.75 Sr 0.25 MnO_3 showed high electrical conductivity (> 100 S/cm). The thermal expansion coefficient of $Pr_{0.75}Sr_{0.25}MnO_3$ and $Nd_{0.75}Sr_{0.25}MnO_3$ were found to be 10.2 x 10^{-6} and 10.7 x 10^{-6} K^{-1} respectively which is very close to that of the electrolyte (YSZ) used in SOFC (10.7 x 10^{-6} K^{-1}). The complex oxides $La_{1-x}Sr_xMnO_3$ (X = 0, 0.1 and 0.2) that are used as the cathode in solid oxide fuel cells have been prepared by Ming *et al.* [46]. Thermodynamic predictions and experiments showed that $La_{1-x}Sr_xMnO_3$ could be prepared via SHS from a mixture of La_2O_3, SrO_2 and Mn using either gaseous oxygen or solid $NaClO_4$ as the oxidant. Partial melting at the high combustion temperature increased the product homogeneity. The electrical conductivity of the product was 180 S/cm at 10273 K in air.

Electron microscopic images and diffraction patterns have been recorded for several crystalline samples of $La_{1-x}Sr_xGa_{1-y}Mg_y\ O_{3-(x+y)/2}$ by Mathews *et al.* [47]. An attempt has been made to identify the microdomain structure using diffraction data obtained from coarse samples and an analogy with stabilized zirconia has been drawn. A homogeneous perovskite oxide $La_{0.5}Sr_{0.5}Ga_{0.2}Fe_{0.8}O_3$ (LSGFO) has been synthesized by Ming *et al.* [48]. The homogeneity and the particle size of the combustion product increased by decreasing the cooling rate. The particle morphology depended upon the gaseous and molten compounds formed as the combustion front passed through the samples. The maximum electrical conductivity of a disk prepared from the SHS powder was 142 S/cm at 6073 K under oxygen pressure of 1 atm. Powders of $La_{0.8}Sr_{0.2}Ga_{1-y}Mg_yO_{3-\delta}$ have been synthesized by both solid oxide/carbonate reaction and citric acid/nitrate combustion processing by Huang *et al.* [49]. The combustion-synthesized powder gave much finer and more homogeneous product. SEM micrograph showed that during sintering, the surface of LSGM samples sintered first, which left standard porosity inside, particularly for samples made from the combustion powders. This difficulty could be overcome by two stage sintering and/or by isostatic pressing. By this technique densification greater than 98% of theoretical was achieved. The maximum conductivity was obtained for the composition $La_{0.8}Sr_{0.2}Ga_{0.875}Mg_{0.125}O_{1-\delta}$ was 0.17 Scm^{-1} at 8273 K. Gonenli *et al.* [50] had synthesized Gd-doped $CaZrO_3$ powders using aqueous solutions of calcium chloride ($CaCl_2 . 2H_2O$) and Zirconium Oxychloride ($ZrOCl_2 . 8H_2O$) in appropriate volumetric amounts.

The ultra fine $LaAlO_3$ powder has been used as the buffer layer on Silicon wafer for $YBa_2Cu_3O_{7-\delta}$ superconductor applications. The microstructure and crystallinity of synthesized $LaAlO_3$ powder were investigated by Nam *et al.* [51] using SEM and XRD. Specific surface area and sintering characteristics of powder were investigated by BET method and dilatometer respectively. From solid-state method, it is difficult to obtain $LaAlO_3$ single phase up to 15273 K, whereas in SHS, it is easy even at 6773 K. Based on the results of the analysis of dilatometric data it is easy to obtain high sintering density (98.97%) in self-sustaining process. The reason is that the average particle size prepared by SHS is of nanocrystalline size and has high specific surface area value (56.54 m^2/g) compared with that of solid-state reaction method. Also $LaAlO_3$ layer on the silver wafer has been achieved by screen printing and sintering method. Eventhough the sintering temperature was 13273 K, the phenomena of silicon diffusion in $LaAlO_3$/Si interphase were not observed. Taspinar *et al.* [52] has successfully synthesized the ferroelectric material $LaAlO_3$ by separate chemical powder preparation technique (i) homogeneous precipitation from aqueous solution containing urea in the presence of nitrate salt and (ii) SHS from aqueous solutions containing CH_4N_2O and the respective nitrate salts of La and Al. The sub micron spherical particles of the precursors were completely converted to pure $LaAlO_3$ at 8773 K in the homogeneous precipitation route. The conversion temperature was observed to be 7773 K, which was the lowest temperature ever reported for the powder synthesis of pure $LaAlO_3$ phase. The materials have been characterized by powder XRD, simultaneous TG/DTA, SEM and Energy dispersive X-ray spectroscopy. Structural refinements by Rietveld analysis showed the $LaAlO_3$ was isostructural with $BaTbO_3$ and had the space group R-3C, in contrast to the previously assumed space group of R-3m for this phase. The atomic position in the structure of $LaAlO_3$ were refined and presented for the first time, with respect to the present space group.

Technologically important lead-based ferro electric niobates of the type A(B'B") (when A is Pb & B' is Fe, Ni, Mg or Zn & B" is Nb) and their solid solution within barium titanate and lead titanate have been prepared by Sekar *et al.* [53] that involves metal nitrate/oxalates and TFTA at a temperature of 4223 K. The thermal effects of niobate perovskites has been investigated at different calcination temperatures, particularly for the determination of density; particle size and surface area. By this technique particles are fine (< 1 μm) and are sinter active at low temperature (10773 K).

Narender *et al.* [54] have prepared $BaTiO_3$ by the addition of $BaTiO_3$ seed particles (50 nm in dia) to a Pb-Mg-Nb-EDTA solution which reduces the formation temperature from 973 K to 873 K during combustion synthesis because of epitaxial effects. The low perovskite formation temperature eliminates the formation of pyrochlore at the surface of the precursor bed and allows for the direct crystallites, ~98%. During combustion synthesis, increase in the nucleation density of the seed particles in the seeder precursor decreases the precursor volume that is associated with each perovskite nucleus and then reduces the PMN particle size from 1 to 0.2 μm. It has been observed that oxidizer/fuel ratio affected the phase formation, morphology and grain size of the $Sr(Fe_{0.5}Ti_{0.5})O_3$ powders by Daniel *et al.* [55].

Maria *et al.* [56] have prepared $La_{1-x}NiO_{3-\delta}$ (x = 0 and 0.1) perovskite combustion product and characterized by XRD, DTA/TG, SEM/TEM, BET and dilatometry. The result shows a high specific surface area value of 4.5 m^2/g which is compared with samples prepared from conventional methods (0.5 m^2/g). Additionally, due to its (conduction band, this material shows a very high electrocatalytic activity particularly in oxygen reduction reaction.

Formation and homogeneity of lanthanum manganite - lanthanum cobaltite solid solution

($LaMn_{1-x}Co_xO_3$) has been confirmed by powder XRD and EDAX by Aruna *et al.* [57]. Linear thermal expansion and electrical conductivity measurements are also carried out. A solution combustion process has been adopted for preparing strontium substituted lanthanum manganite $La_{1-x}Sr_xMnO_3$ (x = 0, 0.1, 0.16, 0.2 and 0.3) using lanthanum nitrate, strontium nitrate and manganese nitrate as oxidizer and oxalyl dihydrazid as fuel at 3273 K in a pre-heated muffle furnace [58]. The cubic $LaMnO_3$ with 36% Mn^{4+} changes to a rhombohedral phase (Mn^{4+}, 28%) on calcination at 10273 K. The surface area and average agglomerated particle size of the manganites were in the range of 12-19 m^2/gm and 5.4-8.0 μm respectively. Strontium substituted lanthanum manganites attained 80% theoretical density after sintering at 13773 K for 4 h and the percentage theoretical density decreased with increasing Sr content. The thermal expansion coefficient of La (Sr) MnO_3 increased with increasing Sr^{2+} content and $La_{0.84}Sr_{0.16}MnO_3$ showed a conductivity value of 202 Scm^{-1} at 9273 K in air.

Spinel structure (AB_2O_4)

The spinel structure consists of a face - centered cubic arrangement of oxygen ions. A unit cell contains 32 O_2 ions; A^{2+} cations occupy 64 tetrahedral sites and B^{3+} cations occupy 32 octohedral sites. The distribution of cations between both sites varies between two limiting cases. The general formula of the "normal" spinel is $(A)[B]_2O_4$ where the parentheses ( ) and [ ] represent tetrahedral and octahedral positions respectively. In the "normal" spinel, A^{2+} cations are located in the tetrahedral sites and the octahedral interstices are occupied by the B^{3+} cations. In the "inverse" spinel, tetrahedral sites are occupied by half of the B^{3+} cations whereas the other half and A^{2+} cations are located in the octahedral sites (formula: $(B)[AB)O_4)$). Structures with intermediate cation distributions exist between these two limiting cases. The formulae of these structures are $(A_{1-x}B_x)[B_{2-x}A_x]O_4$, where ? is the "inversion parameter" ($0 \leq x \leq 1$). The physical and chemical properties of spinels not only depend on the nature of 'A' and 'B' but also depend on the distribution of these cations in the different crystallographic sites [59]. Fig. 2 shows the crystallographic nature of spinel structure [60].

Simple spinels

Xu *et al.* [61] synthesized nanosized $CoFe_2O_4$ spinel and its magnetic properties were elaborately studied. The products with an average grain size

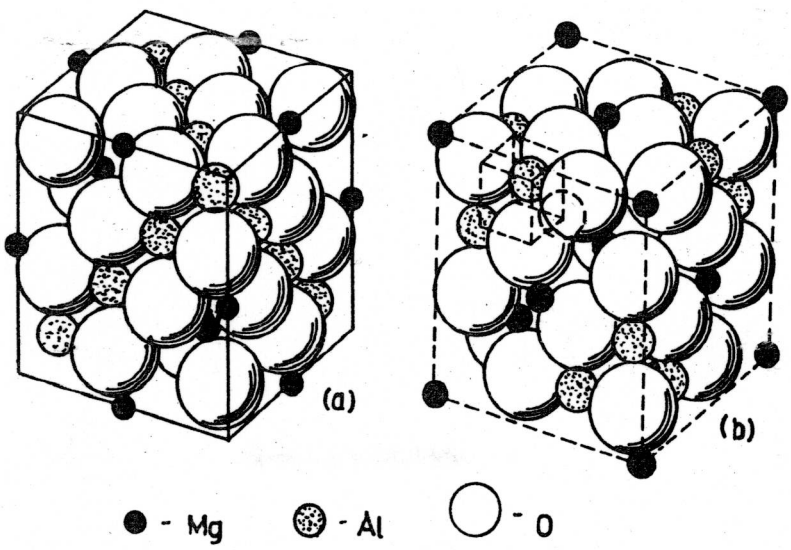

Fig. 2: Spinel Structures ($MgAl_2O_4$)
(a) Normal (b) Unit cell shifted by one-half a cube edge

of 4nm behaved as a super paramagnetic material and have zero coercive force; whereas the samples with an average grain size of 85 nm have the maximal coercive force. The rhombohedral $BaFe_2O_4$ and other ferrites MFe_2O_4 (M = Mg, Co, Ni, Cu, Zn) have been synthesized from iron, cobalt, iron (III) oxide and metal (II) oxides or peroxides by Warren *et al.* [62]. Reactions were carried out in the presence of an external magnetic field of 1.1T. The ratio of tetragonal to cubic phase was observed to increase for $CuFe_2O_4$ by carrying out the reaction in the applied field. All the materials were characterized by XRD, EDXA, SEM and Vibrating Sample Magnetometer (VSM). The combustion synthesized copper ferrite has been prepared using nitrate salts with urea as fuel [63]. The samples were characterized using XRD, FTIR and SEM for the structural and morphological data. The a.c electrical conductivity was measured at room temperature and d.c electrical conductivity was measured from ambient temperature to 10273 K.

$BaFe_2O_4$ and $BaFe_{12}O_{19}$ hexagonal ferrites have been prepared from the corresponding metal nitrates with a reducing agent (ODH) or (TFTA) and were characterized using XRD, TEM for optimizing the best synthesis conditions by Castro *et al.* [64]. The formation of predominantly $MFe_{12}O_{19}$ (M = Sr, Ba) from the metal super oxide (MO_2: M= Sr, Ba), iron and iron powder in thermal initiation of air induced self-propagating reaction with velocity 0.5 mm/sec. The ferrites have been characterized by X- ray powder diffraction (Rietveld analysis), FTIR, VSM magnetization, EDAX/SEM, Electron probe analysis and Mössbaur spectroscopy. The materials showed good quality, coercivity, remanance and hysterisis loops comparable to commercial samples [65]. Preparation of $M_xM_yFe_{12}O_{19}$ (M = Sr, Ba) solid solutions by Ivan *et al.* [66] from a mix of BaO_2, Fe_2O_3 and iron powder under a flow of oxygen inside a quartz tube induced a self-propagation with velocity 2 mm/sec and a temperature of calcination 1248 K. Reactions have also been studied in an applied field of 1.10 T. The effect of changes in the reactant particle size of the iron powder, flow of oxygen and addition of an internal oxidizing agent ($NaClO_4$) has been investigated. The samples have been characterized both before and after annealing by XRD, IR, VSM, SEM, EDXA, Electron Microscope Analysis and Mossbaur spectra. The sintered ferrites showed comparable remanance (σ_v) and maximum magnetization (σ_{max}) when compared with conventionally prepared samples, but significantly lower coercivity [67]. Fig. 3 shows the Mössbaur spectra of conventionally prepared and combustion synthesized $BaFe_{12}O_{19}$ samples. It can be concluded that the combustion synthesized sample gives a higher intensity indicating that the product has well defined structural and crystalline phase. The $BaFe_{12}O_{19}$ has also been prepared by Macro *et al.* [68] using BaO_2, Fe_2O_3 and iron powder.

Subsequent calcination of poly ethylene glycol-metal nitrate precursors has formed a single phase of $LiMn_2O_4$ after calcination above 673 K. From thermal analysis of the precursors, a violent thermal decomposition was indicated by a drastic weight loss accompanied by a sharp and strong exothermic peak. This is caused by an oxidation - reduction reaction between oxidizer and fuel [69]. The physical features of the products have been identified by XPS, XRD, Raman scattering.

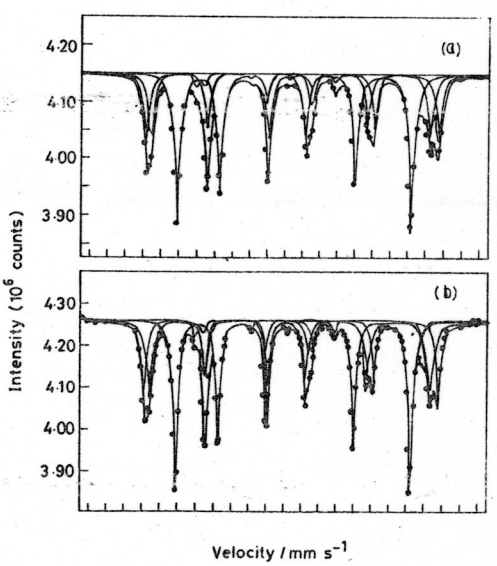

Fig.3. Mössbaur Spectra of $BaFe_{12}O_{19}$ prepared by (a) Conventional method (b) Combustion Synthesis

$Li/LiMn_2O_4$ and $C/LiMn_2O_4$ batteries with non-aqueous organic electrolyte have been fabricated and their performances were studied by Chitra *et al.* [70]. $LiMn_2O_4$ based cathode materials have been fabricated and characterized by XRD as a pure phase. The electrochemical responses of the electrodes have been analyzed by cyclic voltammetry, chronopotentiometry and electrochemical impedance spectroscopy (EIS). CV showed two reversible processes, which is the typical response of $LiMn_2O_4$. The charge-discharge curves showed two plateau with the charge density of 107 mAh/g. From the EIS data Li^+ ion diffusion coefficients have also been determined. The combustion synthesized $LiMn_2O_4$ powder consists of aggregates of ~5 μm, which is smaller crystallites, compared with conventional samples [71]. With varying molar ratio (R) of ethylene glycol (EG) to citric acid (CA) from 0 to 4, the effect of EG content on powder characteristics of $LiMn_2O_4$ were evaluated. With increasing EG content, the homogeneity of the powders are increased and specific surface area are also increased [72].

Alkaline earth indates (AIn_2O_4; A = Mg, Co, Sr and Ba) have been prepared from the carbonate salts [73]. The XRD results and the band gap values were compared with the materials prepared by other samples. From the diffused reflectance spectral measurements of $MgIn_2O_4$, the band gap was found to be 4.3 eV, which is higher than that of indium tin oxide [74]. The conductivity of as prepared samples and that of the H_2 annealed sample of $MgIn_2O_4$ was 1.56×10^{-3} and 5.57 Scm^{-1} respectively. The particle size of the powder sample was found to be 2-3 μm, which is lower than the conventionally prepared samples.

Nanocrystalline metal aluminates MAl_2O_4 (M= Mn, Cu and Zn) have been prepared using corresponding metal acetates, aluminium nitrate, ammonium nitrate and different fuels (eg: urea, carbohydrazide, oxalyl dihydrazide, hexa methylene tetramine and glycine) [75]. The products have been characterized by powder XRD and ^{23}Al MAS NMR spectroscopy. The particulate and morphological properties have been investigated using TEM and SEM techniques. Thermodynamic calculations of the nano crystalline Al_2O_3-MgO have been performed for various compositions from Al_2O_3 rich to the MgO rich side of the phase diagram [76-77]. The as synthesized powders have been characterized by XRD and TEM. The grain sizes calculated from XRD results have been in good agreement with the TEM results. Sub micron calcium aluminate powders have been prepared using metal nitrates-urea mixtures at low temperature and short reaction times by Fumo *et al.* [78]. The effects of the ratio oxidizer/fuel in the redox mixture, phase formation, morphology and grain size have been investigated. Metallic aluminium has been used to produce single phase $MgAl_2O_4$ powder under mild experimental conditions [79-80].

Mixed spinels

The characteristics of combustion synthesized Mn-Zn and Ni-Zn ferrites are found to depend upon the experimental conditions and the content of iron powder [81-82].

Ni-Zn ferrites have been prepared from iron, iron oxide, nickel oxide and zinc oxide at O_2 partial pressure varying between 0.05-5.0 MPa [83]. As the oxygen pressure changed from 0.1-5 MPa, the

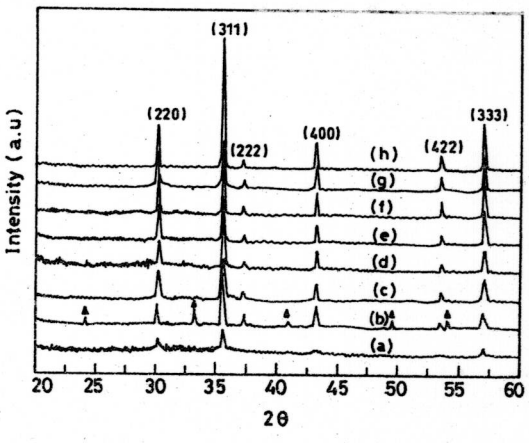

Fig. 4: X-ray diffraction patterns of Ni-Zn ferrite (a) combustion synthesized sample (b) solid state reacted sample sintered at 1123 K/4hr (?-impurity peaks) (c) combustion synthesized sample sintered for 4 hrs at 923 K (d) 1023 K, (e) 1123 K, (f) 1223 K, (g) 1323 K, (h) 1423 K

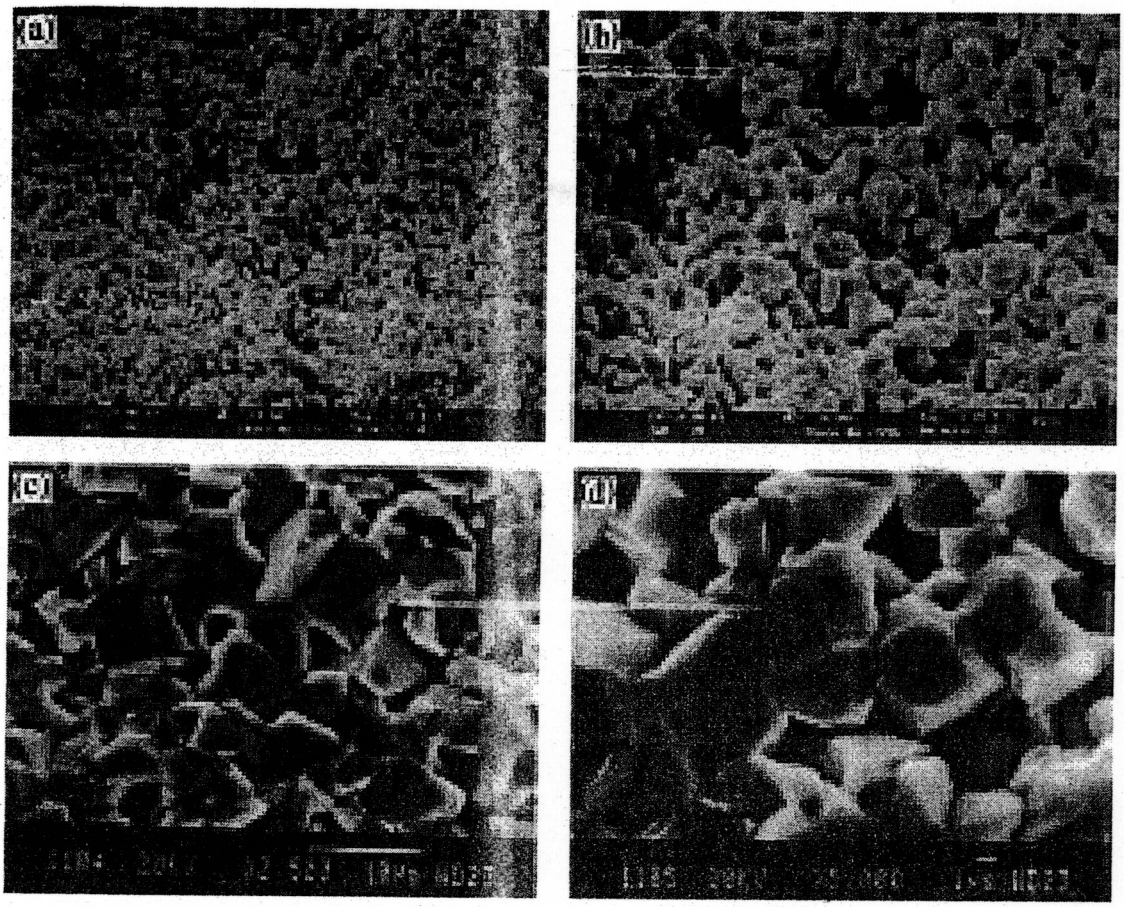

Fig.5. SEM photographs of $Ni_{0.8}Zn_{0.2}Fe_2O_4$ prepared by Flash combustion synthesis at (a) 2500X & (b) 5000X, by Conventional method at (c) 2500X & (b) 5000X

coercive force and the residual magnetization decreased by ≈ 73%, 60% and 32% respectively. The improved magnetic properties are accounted for the enhanced Fe oxidation at a given combustion condition. This method at high O_2 pressure is a useful and efficient method to produce ferrite powders with better magnetic properties than obtained from ceramic method.

Ni-Zn ferrite has been successfully synthesized by microwave induced combustion synthesis [84]. The microwave oven was used in this process and the heat is generated within the sample itself by interaction of microwave with materials within two minutes. The synthesized powder has a particle size of 3-6 μm. It is shown that the combustion synthesized Ni-Zn ferrite annealed at 1123 K exhibits optimum magnetic properties; a saturation magnetization, Ms of 59 emu/g and an intrinsic coercive force, Hc of 135O e. It has been observed that the surface area decreases from 36.1 to 26.5 m^2/ g as the temperature increases from 923 K to 1223 K due to the increase in the particle size.

Fig. 4 shows the X-ray powder diffraction patterns of the Ni-Zn ferrites prepared from both conventional and combustion synthesis with various sintering temperatures. All the patterns show well defined sharp peaks. It can be seen that the conventionally synthesized samples show impurity peaks when compared with the samples prepared from combustion synthesis. The mixed spinel $Ni_{0.35}Zn_{0.65}Fe_2O_4$ has been successfully prepared by Li *et al.* using oxide powders [85-86]. They have studied the influence of iron content, oxygen pressure, grain size and relative density of the raw materials on the combustion product. It

was shown that the combustion temperature (Tc) and combustion wave velocity increased with increase in iron content and the oxygen pressure increase from 0.1 to 0.9 MPa. It has been reported that the increase in grain size and relative density of the raw materials resulted in a decrease of combustion temperature and combustion wave velocity. Hence a conclusion has been derived that the saturation magnetization of the combustion synthesized product is higher (50.37 $Am^2/$ Kg) when compared with the samples prepared by other synthetic methods, like wet chemical method (45.5 $Am^2/$ Kg), solid state reaction method (48.5 $Am^2/$ Kg) and molten salt synthetic method (30.5 $Am^2/$ Kg). R V Mangalaraja *et al.* have prepared the material $Ni_{0.8}Zn_{0.2}Fe_2O_4$ by flash combustion synthesis technique [87]. The magnetic, electrical and dielectric properties of the material were investigated at various sintering temperatures. It has been observed that the dielectric constant (ε') and loss tangent ($\tan \delta$) of the combustion synthesized materials are very low because of the structural homogeneity and molecular level mixing of starting materials as compared with the samples prepared from the conventional method. Higher dielectric constant was resulted from the inhomogeneous nature of dielectric materials. Figs. 5a & 5b show the SEM microphotographs of $Ni_{0.8}Zn_{0.2}Fe_2O_4$ samples prepared from flash combustion synthesis technique and Figs. 5c & 5d by conventional ceramic method. It is seen that the combustion synthesized material has a lower grain size of 2-3 μ m in comparison with the materials obtained by ceramic method.

Pure and chromium substituted lithium ferrites $LiFe_{2.5-x}Cr_xO_4$ ($x \leq 2$), $Li_{0.5}Fe_{2.5-x}Cr_xO_4$ ($0 \leq x \leq 2.0$) has been prepared using Lithium peroxide, Iron oxide, Chromium oxide and Fe or Cr metal powder respectively [88-89]. Reactions were carried out both in zero fields and applied magnetic field of 1.1 T. Rietveld analysis of the powder X-ray data on the sintered sample showed that in all cases a cubic spinel ferrite was produced, which showed a decrease in the lattice parameter with increasing Cr content. Electron microprobe analysis and EDAX showed that the sample was homogeneous and had the expected Fe to Cr ratios. Mössbaur and magnetic hystersis data showed a significant change in sub lattice occupancy and net magnetization with Cr content. Combustion synthesized $MgFe_2O_4$, chromium substituted magnesium zinc ferrite $Mg_{0.5}Zn_{0.5}Fe_{2-x}Cr_xO_4$ ($0 \leq x \leq 1.5$), pure and chromium substituted Barium ferrite $BaFe_{12-x}Cr_xO_{19}$ ($0 \leq x \leq 1.5$), Lithium ferrite ($Li_{0.5}Fe_{2.5}O_4$) and Magnesium Zinc ferrite ($Mg_{0.5}Zn_{0.5}Fe_2O_4$) have been characterized before and after annealing by XRD, FTIR, VSM, EDAX/SEM and Mössbaur spectroscopy [90-93].

CONCLUSION

Combustion synthesis has been found to be a suitable and simple method to synthesize different classes of compounds especially perovskites and spinels. It can be adopted to tailor make materials with preset properties, structures and substitution either in A or B site ions. This will enable one to provide apt materials to meet the challenges faced by the rapid advancements in science and technology where newer materials with stringent quality and serviceability are required. It is hoped that the combustion synthesis will serve the materials scientists better in the coming years.

REFERENCES

1. Ping Yang, Meng Kai Li and De Hong Chen, *Materials Science and Engg,* Article in press (2002)
2. E H Walker Jr, J W Owens and Don Walker, *Mat Res Bull,* **37** (2002) 1041
3. A S Albuquerque, J D Ardission and W A A Macedo, *J Magn Magn Mater,* **192** (1999) 277
4. Hui-Qin Ling, Ai-Dong Li and Nai-Ben Ming, *Mat Chem and Phys,* **75** (2002) 170
5. H Taguchi, S Yamada and K Tabata, *Mat Res Bull,* **37** (2002) 69
6. Yang-Kook Sun, Jn-Hwan Oh and Kwang Yul Kim, *Ind Engg Chem Res,* **36** (1997) 4839
7. Y Shi, J Ding and J Wang, *J Magn Magn Mat,* **205** (1999) 249
8. Alexander A Kamnev and Mira Ristic, *J Molecular Structure,* **408/409** (1997) 301

9. Zhizhan Chen, Erwei Shi and Weizhuo Zhong, *Mat Letters,* **56** (2002) 601
10. Changhura An, Kaibin Tang and Yitai Qian, *Mat Res Bull,* **37** (2002) 1791
11. S D Sartale and C D Lokhande, *Mater Chem and Phys,* **70** (2001) 274
12. S D Sartale and C D Lokhande, *Ind J Engg & Materials Sci,* **7** (2000) 404
13. V Surve and V Puri, *Bull Electrochem,* **14** (1998) 151
14. Hung-Pin Li, *Materials Chem and Phy,* **49** (1997) 150
15. A G Merzhanov, *Int J Self Propag High-Temp Synth,* **2** (1993) 113
16. C R Bowen and B Derby, *Acta Metall Mater,* **43** (1995) 3903
17. C R Bowen and B Derby, *Brit Ceram Trans,* **96** (1997) 25
18. H C Yi and J J Moore, *J Mater Sci,* **25** (1990) 1159
19. J J Moore and H J Feng, *Prog Mater Sci,* **39** (1995) 243
20. J A Puszynski and F D S Marquin, *Environ Res Forum,* **1** (1996) 329
21. A V Khachoyan, E V Zabotina and N A Belkina, *Int J Self-Propag High Temp Synth,* **5** (1996) 305
22. H Wang, J Han and S Du, *Gongneng Cailiao,* **28** (1997) 115
23. K C Patil, Ekambaram and Sambandan, *Curr Opi Solid State Mater Sci,* **2** (1997) 158
24. A Varma, A Rogachev and Hwang Stephan, *Advanced Chem Eng,* **24** (1998) 79
25. Y Li, J Han and S Du, *Gongneng Cailiao,* **30** (1999) 598
26. M R Morelli, B Derby and R J Brook, *J Ceramica,* **42** (1996) 435
27. C H Jung, H K Park and Y Y Park, *Yoop Hakhoechi,* **35** (1998) 1078
28. K Zupan and Kovine, *Zlitine Technol,* **31** (1997) 75
29. Xiwei Qi, Ji Zhou and Longtu Li, *Mat Chem Phys,* **78** (2002) 25
30. J W Stevanson, K Hasinka and T R Armsrong, *Proc Electrochem Soc,* **99-19** (SOFC VI) (1999) 275
31. M D Aguas and I P Parkin, *J Mater Sci Lett,* **20** (2001) 57

32. X Zhu, K Zhav and Su Yunsheng, *Int J Self-Propag High Temp Synth,* **6** (1996) 47
33. J Poth, R Haberkorn and H P Beck, *J Eur Ceram Soc,* **20** (2000) 707
34. J Poth, R Haberkorn and H P Beck, *J Eur Ceram Soc,* **20** (2000) 715
35. S Mao, Y Cai and J Zhao, *Gongneng Cailiao,* **29** (1998)110
36. A M Azad, L L N Shyan and C H Wee, *Ceram Int,* **26** (2000) 685
37. A M Azad and Hon Neechen, Li, J Han and S Du, *Gongneng Cailiao,* **30** (1999) 598; *J Alloys Compd,* **270** (1998) 95
38. Q Ming, M Nersesyan and D Luss, *Combust Sci Technol,* **35** (1997) 1078
39. A A Shiryaev, M D Nerseyan and D Luss, *J Mater Synth Process,* **7** (1999) 83
40. K Zupan, A Bencan and B Novosel, *1999 Kovine Zlitine Technol,* **33** (1999) 55
41. Q Ming, M Nersesyan and D Luss, *Proc Electrochem Soc,* **99-19** (1999) (SOFC VI) 474
42. M V Kuznetsov, Barguin and I P Parkin, *J Phys D Appl Phys,* **32** (1999) 2590
43. M V Kuznetsov and I P Parkin, *Mater Sci Forum,* **321** (2000) 779
44. M V Kuznetsov, A P Quentinand G M Yury, *J Mater Chem,* **11** (2001) 854
45. S T Aruna, M Muthuraman and K C Patil, *Solid State Ionics,* **120** (1999) 275
46. Q Ming, M Nersesyan and A A Shiryaev, *J Mater Sci,* **35** (2000) 3599
47. T Mathews and J R Sellar, *Solid State Ionics,* **135** (2000) 411
48. Q Ming, M Nersesyan and Y L Yang, *Solid State Ionics,* **122** (1999) 411
49. P N Huang, A Petric and D Ghosh, *Proc Electrochem Soc,* **99-19** (SOFC VI) (1999) 285
50. I E Gonenli and A C Tas, *Ceram Trans,* **109** (2000) 153
51. H D Nam, W S Choi and S Park, *Yoop Hok Hoechi,* **36** (1999) 203
52. E Taspinar and A C Tas, *J Amer Ceram Soc,* **80** (1997)133
53. M M A Sekar and H Aravind, *J Amer Ceram Soc,* **81** (1998) 380
54. Y Narendar and G L Messing, *J Amer Ceram Soc,* **82** (1999)1659
55. A F Daniel, F R Jurado and J R Frade, *Mater Res Bull,* **32** (1997) 1459
56. Maria T Colomer, Daniel A Fumo and Ana M Segadaes, *J Mater Chem,* **9** (1999) 2505
57. S T Aruna, M Muthuraman and K C Patil, *Mater Res Bull,* **35** (2000) 289
58. S T Aruna, M Muthuraman and K C Patil, *J Mater Chem,* **7** (1997) 2499

59. L Schreyeck, A Wlosik and H Fuzellier, *J Mater Chem*, **11** (2001) 483
60. E J W Verway and E L Heilmann, *J Chem and Phys*, **15(4)** (1947) 174
61. Xu Zhigarg, Cheng and Yan Chuhua, *Chin Sci Bull*, **46** (2001) 384
62. Warren B Cross, Louise Affleck and Quentin A Pankhurst, *J Mater Chem*, **9** (1999) 2545
63. R Kalai Selvan, C O Augustin, L John Berchmans and R Saraswathi, *Mater Res Bull*, **38** (2003) 41
64. S Castro, M Gayoso and C Rodriquez, *J Mater Chem*, **134** (1997) 227
65. S K Mishra, L C Pathak and V Rao, *Mater Lett*, **32** (1997) 137
66. Ivan P Parkin, Gareth E Elwin and G M Yuri, *J Mater Chem*, **32** (1998) 573
67. Louise Affleck, Macro D Aguas and Maxim V Kuznetsov, *J Mater Chem*, **10** (2000) 1925
68. Macro D Aguas, Louise Affleck and A A Jos, *J Mater Chem*, **10** (2001) 235
69. Park, Hyu-Bum, Y S Hong and Kim Si- Foong, *Bull Korean Chem Soc*, **18** (1997) 612
70. S Chitra, P Kalyani and M Eddrief, *J Electo Ceram*, **3** (1999) 433
71. Lee, Ki-Min, Choi, Heon-Jin, Lee and June-Gunn, *J Mater Sci Letts*, **20** (2001) 1309
72. Y S Han, J T Son and H T Jung, *Han'guk Seramik Hakhoechi*, **38** (2001) 301
73. S E Dali, Sundar VVVS Sai and M J Chockalingam, *J Mater Sci Lett*, **17** (1998) 619
74. S Esther Dali and M J Chockalingam, *Mater Chem and Phys*, **70** (2001) 73
75. T Mimani, *J Alloys Compds*, **315** (2001) 123
76. S Bhaduri, E Zhou and S B Bhaduri, *Ceram Eng Sci Proc*, **18** (1997) 645
77. S Bhaduri, S B Bhaduri and K A Prisbrey, *J Mater Res*, **14** (1999) 3571
78. D A Fumo, M B Morelli and A M Segadaes, *Mat Res Bull*, **31** (1996) 1243
79. Lim Rooi Ping, Abdul-Majeed Azad and Teng Wan Dung, *Mat Res Bull*, **36** (2001)1417
80. L B Kong, J Ma and H Huang, *Mat Lett*, **56** (2002) 238
81. W Lee, Kim, Dong-Hoon and Kim Brung-Kyu, *Chawon Risaikring*, **5** (1996) 37
82. Y Li, J P Zhao and H Xian, *Gongneng Cailiao*, **32** (2001) 248
83. Choi Yong, Cho Namihn and Y D Hahn, *J Mater Sci Mater Electron*, **11** (2000) 25
84. Yen-Pei and Cheng-Hsiung Lin, *J Magn Magn Mater*, **251** (2002) 583
85. Y Li, J Zhao and J Hen, *Bull Mater Sci*, **25** (2002) 263
86. Y Li, J Zhao and J Hen, *Mat Res Bull*, **37** (2002) 583
87. R V Mangalaraja, S Ananthakumar, P Manohar and F D Gnanam, *J Magn Magn Mater*, **253** (2002) 56
88. B L Fernandez, M V Kuznetsov and P Ivan, *Int J Inorg Mater*, **1** (1999) 311
89. Maxim V Kuznetsov, A P Quentinand and Ivan P Parkin, *J Phys D Appl Phys*, **31** (1998) 2886
90. Maxim V Kuznetsov, A P Quentin and Ivan P Parkin, *J Mater Chem*, **8** (1998) 2701
91. Ivan P Parkin, Maxim V Kuznetsov and A P Quentin, *J Mater Chem*, **9** (1999) 273
92. Ivan P Parkin, A P Quentin and Maxim V Kuznetsov, *J Mater Chem*,**11** (2001)193
93. C H Jung, Y Y Park and J Y Park, *J Ceram Soc*, **6** (2000)47